Eur. Phys. J. C 46, 357–365 (2006)
Digital Object Identifier (DOI) 10.1140/epjc/s2006-02477-x

THE EUROPEAN PHYSICAL JOURNAL C

Factorizable electroweak $\mathcal{O}(\alpha)$ corrections for top quark pair production and decay at a linear e^+e^- collider

K. Kołodziej[1,a], A. Staroń[1,b], A. Lorca[2,c], T. Riemann[2,d]

[1] Institute of Physics, University of Silesia, ul. Uniwersytecka 4, 40007 Katowice, Poland
[2] Deutsches Elektronen-Synchrotron DESY, Platanenallee 6, 15738 Zeuthen, Germany

Received: 17 October 2005 / Revised version: 19 December 2005 /
Published online: 24 March 2006 –

Abstract. We calculate the standard model predictions for top quark pair production and decay into six fermions at a linear e^+e^- collider. We include the factorizable electroweak $\mathcal{O}(\alpha)$ corrections in the pole approximation and QED corrections due to the initial state radiation in the structure function approach. The effects of the radiative corrections on the predictions are illustrated by showing numerical results for two selected six-fermion reactions $e^+e^- \to b\nu_\mu\mu^+\bar{b}\mu^-\bar{\nu}_\mu$ and $e^+e^- \to b\nu_\mu\mu^+\bar{b}d\bar{u}$.

1 Introduction

Precise measurements of top quark pair production

$$e^+e^- \to t\bar{t} \tag{1}$$

at the threshold and in the continuum region will belong to the basic physics program of the future international linear collider (ILC) [1]. In order to fully profit from these high precision measurements, one has to bring theoretical predictions to at least the same, or preferably better, precision, which obviously requires taking into account radiative corrections. The latter should be calculated not only for the on-shell production process (1). Due to their large widths, the t-quark and $\bar{t}$-quark of reactions (1) almost immediately decay into bW^+ and $\bar{b}W^-$, respectively, and the W-bosons subsequently decay into two fermions each, thus constituting six-fermion reactions of the form

$$e^+e^- \to bf_1\bar{f}_1'\bar{b}f_2\bar{f}_2', \tag{2}$$

where $f_1, f_2' = \nu_e, \nu_\mu, \nu_\tau, u, c$ and $f_1', f_2 = e^-, \mu^-, \tau^-, d, s$. Typical lowest order Feynman diagrams of reaction (2) are shown in Fig. 1.

As decays of the top and antitop take place before toponium resonances can form, the standard model (SM) predictions for reaction (1) can be obtained with the perturbative method. The QCD predictions for reaction (1) in the threshold region were obtained in [2] and then improved by calculation of the next-to-next-to-leading order QCD corrections [3], and by including the effects of initial state radiation and beamstrahlung [4]. The $\mathcal{O}(\alpha\alpha_s)$ [5–7] and $\mathcal{O}(\alpha\alpha_s^2)$ [8] corrections to the subsequent top decay into a W boson and a b quark are also known. In the continuum above the threshold, the QCD predictions for reaction (1) are known to the order of α_s^2 [9] and the electroweak (EW) corrections to one-loop order [10–12], including the hard bremsstrahlung corrections [11, 13]. The QCD and EW corrections are large, typically of $\mathcal{O}$ (10%). The orders α_s [15] and α_s^2 QCD, and EW corrections have been combined in [16]. Quite recently, the EW radiative corrections to (1) have been recalculated with the program TOPFIT [11, 12] and thoroughly compared with results of other calculations, with hard bremsstrahlung [17] and without it [18]. Finally, the radiative corrections to W decays into fermion pairs, which also must be taken into account, are also known [19–21].

At tree level, reactions (2) can be studied with a Monte Carlo (MC) program eett6f [22, 23] or with any other MC program dedicated to the six fermion reactions, such as SIXPHACT [24], SIXFAP [25], LUSIFER [26], or any of multi-purpose generators, such as AMEGIC [27], GRACE [28]/BASES [29], MADGRAPH [30]/MADEVENT [31], PHEGAS [32]/HELAC [33], or WHIZARD [34]/COMPHEP [35], MADGRAPH [30], or O'MEGA [36]. Thorough comparison of the lowest order predictions for several different channels of (2) obtained with AMEGIC++, eett6f, LUSIFER, PHEGAS, SIXFAP and WHIZARD have been performed within the framework of the Monte Carlo generators group of the ECFA/DESY workshop [37]. A survey of SM cross sections of all six fermion reactions with up to four quarks in the limit of massless fermions (other than the top quark), has been done in [26]. The latter also contains a fine tuned comparison of both the lowest order and lowest order plus ISR results, obtained in

[a] e-mail: kolodzie@us.edu.pl
[b] e-mail: staron@server.phys.us.edu.pl
[c] e-mail: alorca@ifh.de
[d] e-mail: Tord.Riemann@desy.de

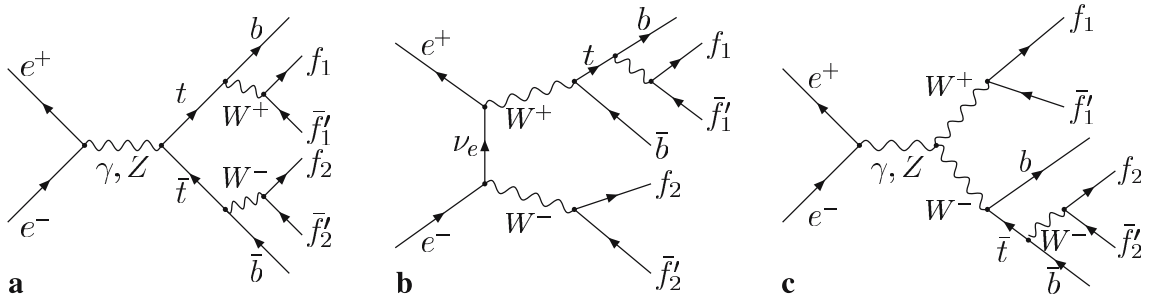

Fig. 1. Examples of Feynman diagrams of reaction (2): **a** 'signal', **b** and **c** 'background' diagrams

the structure function approach, between LUSIFER and WHIZARD.

Concerning radiative corrections to the six-fermion reactions (2), the situation is less advanced. Already at the tree level, any of the reactions receives contributions from typically several hundred Feynman diagrams, e.g. in the unitary gauge, with neglect of the Higgs boson couplings to fermions lighter than the b quark, reactions $e^+e^- \to b\nu_\mu\mu^+\bar{b}d\bar{u}$, $e^+e^- \to b\nu_\mu\mu^+\bar{b}\mu^-\bar{\nu}_\mu$, and $e^+e^- \to bu\bar{d}b\bar{d}\bar{u}$ receive contributions from 264, 452, and 1484 Feynman diagrams, respectively. Hence, the calculation of the full $\mathcal{O}(\alpha)$ radiative corrections to any of reactions (2) seems not to be feasible at present. Therefore, in the present note we will take a step towards improving precision of the lowest order predictions for (2) by including leading radiative effects, such as initial state radiation (ISR) and factorizable EW radiative corrections to the process of the on-shell top quark pair production (1), to the decay of the t ($\bar{t}$) into bW^+ ($\bar{b}W^-$) and to the subsequent decays of the W-bosons. We will illustrate an effect of these corrections by showing numerical results for the two selected six-fermion reactions

$$e^+e^- \to b\nu_\mu\mu^+\bar{b}\mu^-\bar{\nu}_\mu \tag{3}$$

and

$$e^+e^- \to b\nu_\mu\mu^+\bar{b}d\bar{u}\,. \tag{4}$$

2 Calculation scheme

We calculate the ISR and the factorizable SM corrections for the reaction

$$\begin{aligned} e^+(p_1,\sigma_1)e^-(p_2,\sigma_2) \to b(p_3,\sigma_3)f_1(p_4,\sigma_4)\bar{f}_1'(p_5,\sigma_5) \\ \times \bar{b}(p_6,\sigma_6)f_2(p_7,\sigma_7)\bar{f}_2'(p_8,\sigma_8)\,, \end{aligned} \tag{5}$$

where the particle momenta and helicities have been indicated in the parentheses, according to the following formula:

$$\begin{aligned} \mathrm{d}\sigma = \int_0^1 \mathrm{d}x_1 \int_0^1 \mathrm{d}x_2\, \Gamma_{ee}^{LL}\left(x_1,Q^2\right)\Gamma_{ee}^{LL}\left(x_2,Q^2\right) \\ \mathrm{d}\sigma_{\mathrm{Born+FEWC}}\left(x_1p_1,x_2p_2\right)\,, \end{aligned} \tag{6}$$

where x_1p_1 (x_2p_2) are the four momenta of the positron (electron) after emission of a collinear photon. The structure function $\Gamma_{ee}^{LL}\left(x,Q^2\right)$ is given by (67) of [38], with the 'BETA' choice for non-leading terms. The splitting scale Q^2, which is not fixed in the LL approximation is chosen to be $s=(p_1+p_2)^2$. By $\mathrm{d}\sigma_{\mathrm{Born+FEWC}}$ we denote the cross section including the factorizable EW $\mathcal{O}(\alpha)$ corrections

$$\begin{aligned} &\mathrm{d}\sigma_{\mathrm{Born+FEWC}} \\ &\quad = \frac{1}{2s}\left\{\overline{|M_{\mathrm{Born}}|^2} + 2\mathrm{Re}\overline{\left(M_{t\bar{t}}^*\delta M_{t\bar{t},\mathrm{FEW}}\right)}\right\}\mathrm{d}\Phi_{6f}\,, \end{aligned} \tag{7}$$

where M_{Born} is the matrix element of reaction (5) obtained with the complete set of the lowest order Feynman diagrams, $M_{t\bar{t}}$ and $\delta M_{t\bar{t},\mathrm{FEW}}$ are, respectively, the lowest order amplitude of the 'signal' Feynman diagram of Fig. 1a and the corresponding factorizable EW $\mathcal{O}(\alpha)$ correction, both in the pole approximation. The overlines in (7) denote, as usual, an initial state particle spin average and a sum over final state particle polarizations, and $\mathrm{d}\Phi_{6f}$ is the Lorentz invariant six-particle phase space element. The basic phase space parameterizations used in the program are given by (7)–(9) of [22]. The corrections that we take into account in $\delta M_{t\bar{t},\mathrm{FEW}}$ are illustrated diagrammatically in Fig. 2.

In the pole approximation, the polarized lowest order amplitude $M_{t\bar{t}}$ and the one-loop correction $\delta M_{t\bar{t},\mathrm{FEW}}$ of (7) can be expressed analytically as follows:

$$\begin{aligned} M_{t\bar{t}}^{\sigma_1\sigma_2;\sigma_3\dots\sigma_8} &= \frac{1}{D_t\left(p_{345}\right)D_t\left(p_{678}\right)} \\ &\times \sum_{\sigma_t,\sigma_{\bar{t}}} M_{e^+e^-\to t\bar{t}}^{\sigma_1\sigma_2;\sigma_t\sigma_{\bar{t}}} M_{t\to bf_1f_1'}^{\sigma_t;\sigma_3\sigma_4\sigma_5} M_{\bar{t}\to\bar{b}f_2f_2'}^{\sigma_{\bar{t}};\sigma_6\sigma_7\sigma_8} \end{aligned} \tag{8}$$

$$\begin{aligned} \delta M_{t\bar{t}}^{\sigma_1\sigma_2;\sigma_3\dots\sigma_8} &= \frac{1}{D_t\left(p_{345}\right)D_t\left(p_{678}\right)} \\ &\times \sum_{\sigma_t,\sigma_{\bar{t}}} \Big[\delta M_{e^+e^-\to t\bar{t}}^{\sigma_1\sigma_2\sigma_t,\sigma_{\bar{t}}} M_{t\to bf_1f_1'}^{\sigma_t;\sigma_3\sigma_4\sigma_5} M_{\bar{t}\to\bar{b}f_2f_2'}^{\sigma_{\bar{t}};\sigma_6\sigma_7\sigma_8} \\ &+ M_{e^+e^-\to t\bar{t}}^{\sigma_1\sigma_2;\sigma_t\sigma_{\bar{t}}} \delta M_{t\to bf_1f_1'}^{\sigma_t\sigma_3\sigma_4\sigma_5} M_{\bar{t}\to\bar{b}f_2f_2'}^{\sigma_{\bar{t}};\sigma_6\sigma_7\sigma_8} \\ &+ M_{e^+e^-\to t\bar{t}}^{\sigma_1\sigma_2;\sigma_t\sigma_{\bar{t}}} M_{t\to bf_1f_1'}^{\sigma_t;\sigma_3\sigma_4\sigma_5} \delta M_{\bar{t}\to\bar{b}f_2f_2'}^{\sigma_{\bar{t}};\sigma_6\sigma_7\sigma_8}\Big]\,, \end{aligned} \tag{9}$$

where the lowest order t and $\bar{t}$ decay amplitudes and the corresponding one-loop corrections read

$$M_{t\to bf_1f_1'}^{\sigma_t\sigma_3\sigma_4\sigma_5} = \frac{1}{D_W\left(p_{45}\right)}\sum_{\lambda_{W^+}} M_{t\to bW^+}^{\sigma_t\sigma_3\lambda_{W^+}} M_{W^+\to f_1f_1'}^{\lambda_{W^+}\sigma_4\sigma_5}\,, \tag{10}$$

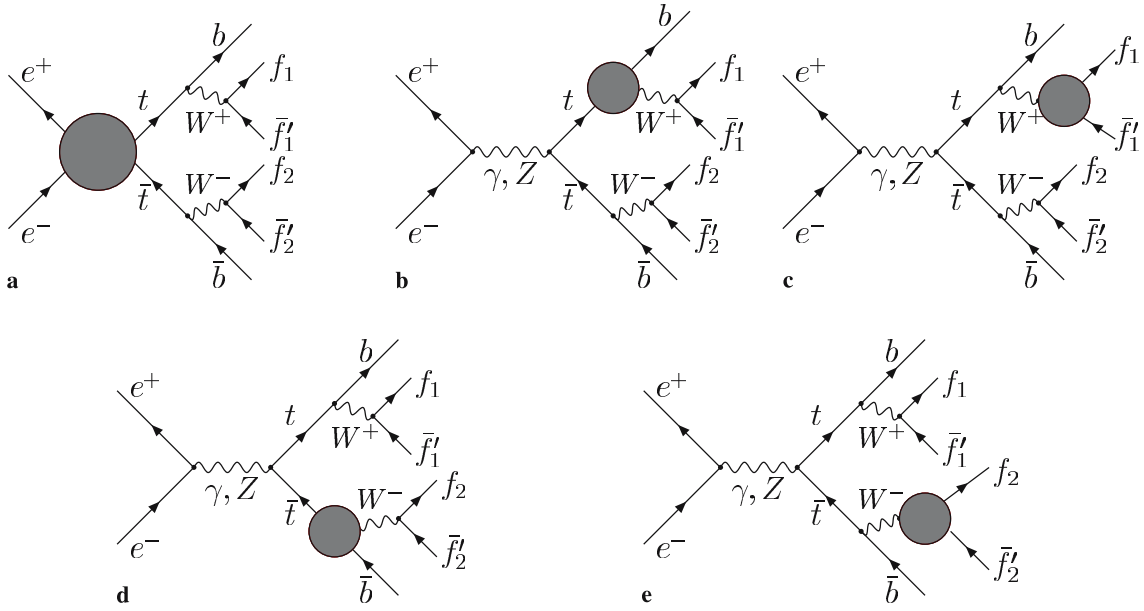

Fig. 2. Factorizable EW corrections to reaction (2)

$$M^{\sigma_{\bar t}\sigma_6\sigma_7\sigma_8}_{\bar t\to\bar b f_2 f_2'} = \frac{1}{D_W\,(p_{78})} \sum_{\lambda_{W^-}} M^{\sigma_{\bar t}\sigma_6\lambda_{W^-}}_{\bar t\to\bar b W^-}\, M^{\lambda_{W^-}\sigma_7\sigma_8}_{W^-\to f_2 f_2'}\,, \quad (11)$$

$$\delta M^{\sigma_t\sigma_3\sigma_4\sigma_5}_{t\to b f_1 f_1'} = \frac{1}{D_W\,(p_{45})} \sum_{\lambda_{W^+}} \left[\delta M^{\sigma_t\sigma_3\lambda_{W^+}}_{t\to bW^+}\, M^{\lambda_{W^+}\sigma_4\sigma_5}_{W^+\to f_1 f_1'} + M^{\sigma_t\sigma_3\lambda_{W^+}}_{t\to bW^+}\, \delta M^{\lambda_{W^+}\sigma_4\sigma_5}_{W^+\to f_1 f_1'}\right], \quad (12)$$

$$\delta M^{\sigma_{\bar t}\sigma_6\sigma_7\sigma_8}_{\bar t\to\bar b f_2 f_2'} = \frac{1}{D_W\,(p_{78})} \sum_{\lambda_{W^-}} \left[\delta M^{\sigma_{\bar t}\sigma_6\lambda_{W^-}}_{\bar t\to\bar b W^-}\, M^{\lambda_{W^-}\sigma_7\sigma_8}_{W^-\to f_2 f_2'} + M^{\sigma_{\bar t}\sigma_6\lambda_{W^-}}_{\bar t\to\bar b W^-}\, \delta M^{\lambda_{W^-}\sigma_7\sigma_8}_{W^-\to f_2 f_2'}\right]. \quad (13)$$

In (8)–(13), σ_t, $\sigma_{\bar t}$ and λ_{W^+}, λ_{W^-} denote polarizations of the intermediate top quarks and W bosons, which are treated as on-shell particles, except for that they keep their actual off-shell momenta

$$\begin{aligned} p_{345} &= p_3+p_4+p_5\,,\; p_{678} = p_6+p_7+p_8\,,\\ p_{78} &= p_7+p_8\,,\; p_{45} = p_4+p_5 \end{aligned} \quad (14)$$

in the denominators $D_t\,(p)$ and $D_W\,(p)$ of their propagators

$$\begin{aligned} D_t\,(p) &= p^2 - m_t^2 + i m_t \Gamma_t\,,\\ D_W\,(p) &= p^2 - m_W^2 + i m_W \Gamma_W\,. \end{aligned} \quad (15)$$

The fixed widths Γ_t and Γ_W of (15) are calculated in the program for a given set of initial parameters. They are set to their SM lowest order values, $\Gamma_t^{(0)}$ and $\Gamma_W^{(0)}$, for the Born cross sections, or they include radiative corrections of the same kind as those included in the numerators of (9), (12) and (13) for the radiatively corrected cross sections.

While explaining further the notation of (8)–(13) we will suppress the polarization indices. $M_{e^+e^-\to t\bar t}$ and $\delta M_{e^+e^-\to t\bar t}$ are the lowest order and the EW one-loop amplitudes of the on-shell top quark pair production process (1). They can be decomposed into a basis composed of the following invariant amplitudes

$$\begin{aligned} \mathcal{M}_{1,\,ab} &= \bar v(p_1)\;\gamma^\mu\, g_a\, u(p_2)\;\bar u(k_t)\gamma_\mu\, g_b\, v(k_{\bar t})\,, g_a, g_b = \mathbb{1}, \gamma_5\,,\\ \mathcal{M}_{3,11} &= -\bar v(p_1)\;\not k_t\, u(p_2)\;\bar u(k_t) v(k_{\bar t})\,,\\ \mathcal{M}_{3,51} &= -\bar v(p_1)\;\not k_t\,\gamma_5 u(p_2)\;\bar u(k_t) v(k_{\bar t})\;. \end{aligned} \quad (16)$$

The projected four momenta $k_t, k_{\bar t}$ of the on-shell top- and antitop quark of (16), as well as the four momenta k_{W^+}, k_{W^-} of the on-shell W-bosons and the four momenta $k_3, \ldots, k_8$ of the decay fermions, which are used later, have been obtained from the four momenta of the final state fermions $p_3, \ldots, p_8$ of reaction (2) with the projection procedure described in Appendix A.

In terms of invariant amplitudes (16), the lowest order amplitude of (1) reads

$$M_{e^+e^-\to t\bar t} = \sum_{a,b=1,5} \mathrm{F}^{ab}_{1B}\;\mathcal{M}_{1,ab}\,, \quad (17)$$

where the four Born form factors F^{ab}_{1B} are given by

$$\begin{aligned} \mathrm{F}^{11}_{1B} &= \frac{e_W^2\,(\chi_Z v_e v_t + Q_e Q_t)}{s}\,, \quad \mathrm{F}^{51}_{1B} = -\frac{e_W^2 \chi_Z v_t a_e}{s}\,,\\ \mathrm{F}^{15}_{1B} &= -\frac{e_W^2 \chi_Z v_e a_t}{s}\,, \qquad\qquad \mathrm{F}^{55}_{1B} = \frac{e_W^2 \chi_Z a_e a_t}{s}\,. \end{aligned} \quad (18)$$

In (18), e_W is the effective electric charge, $e_W = \sqrt{4\pi\alpha_W}$, with

$$\alpha_W = \frac{\sqrt{2} G_\mu m_W^2 \sin^2\theta_W}{\pi} \text{ and } \sin^2\theta_W = 1 - \frac{m_W^2}{m_Z^2}\,. \quad (19)$$

The Z-boson propagator is contained in the factor

$$\chi_Z = \frac{1}{4\sin^2\theta_W\cos^2\theta_W}\frac{s}{s-m_Z^2+im_Z\Gamma_Z}\,, \tag{20}$$

and we have used the following conventions for couplings of the electron and top quark to a photon and a Z-boson

$$\begin{aligned} &Q_e=-1, Q_t=\frac{2}{3}\,, a_e=-a_t=-\frac{1}{2}\,,\\ &v_f=a_f\left(1-4\left|Q_f\right|\sin^2\theta_W\right)\,, f=e,t\,. \end{aligned} \tag{21}$$

We have introduced a constant Z-boson width Γ_Z in (20), in a similar way as Γ_t and Γ_W have been introduced in (15), although the Z-boson propagator in the e^+e^- annihilation channel never becomes resonant in the CMS energy range above the $t\bar{t}$-pair production threshold. Generally speaking, the constant width Γ of an unstable particle is introduced into the lowest order matrix elements by replacing its mass with the complex mass parameter

$$m^2 \to m^2 - im\Gamma \tag{22}$$

in the corresponding propagator, both in the s-channel and t-channel, while keeping the electroweak mixing parameter $\sin^2\theta_W$ of (19) real. This approach is usually referred to in the literature as the fixed width scheme (FWS). The approach, in which m_W^2 and m_Z^2 are replaced with their complex counterparts according to (22), also in $\sin^2\theta_W$ of (19) is, on the other hand, referred to as the complex mass scheme [39]. The latter has the advantage that it preserves Ward identities. Let us note that in (8)–(13), substitution (22) is done only in the denominators of the top quark and W-boson propagators and not in the one-loop amplitudes. Also the sums over the top quark and W-boson polarizations result in the numerators of the corresponding propagators with real masses. However, this does not violate the substitution rule of (22), as the amplitudes of (8)–(13) constitute the factorizable one-loop correction term in (7).

The EW one-loop amplitude of (1) reads

$$\delta M_{e^+e^-\to t\bar{t}} = \sum_{a,b=1,5}\hat{F}_1^{ab}\mathcal{M}_{1,ab} + \hat{F}_3^{11}\mathcal{M}_{3,11} + \hat{F}_3^{51}\mathcal{M}_{3,51}\,, \tag{23}$$

with the six independent form factors: $\hat{F}_1^{ab}, a,b=1,5$, $\hat{F}_3^{11}$ and $\hat{F}_3^{51}$, which are calculated numerically with the program `topfit` [11,12] that is tailored to a subroutine of a new version of `eett6f`. Note that a factor i has been omitted on the left-hand side of (16) compared to [11]. Keeping it would result in an extra minus sign on the right-hand sides of (8) and (9), as we neglect the i factor in every vertex and propagator and, consequently, the resulting common $+i$ factor for every Feynman diagram in the present work. The flags in `topfit` switch off all photonic corrections there, including the running of the electromagnetic coupling. This means that only the genuine weak corrections will contribute.

In order to fix normalization, we give the formula for the EW one-loop corrected cross section $\mathrm{d}\sigma_{e^+e^-\to t\bar{t}}$ of the on-shell top production (1)

$$\begin{aligned} \mathrm{d}\sigma_{e^+e^-\to t\bar{t}} &= \frac{1}{2s}\\ &\times\left\{\left|M_{e^+e^-\to t\bar{t}}\right|^2 + 2\mathrm{Re}\left(M^*_{e^+e^-\to t\bar{t}}\delta M_{e^+e^-\to t\bar{t}}\right)\right\}\mathrm{d}\Phi_{2f}\,, \end{aligned} \tag{24}$$

where the matrix elements $M_{e^+e^-\to t\bar{t}}$ and $\delta M_{e^+e^-\to t\bar{t}}$ are given by (17) and (23), and $\mathrm{d}\Phi_{2f}$ is the Lorentz invariant two-particle phase space element

$$\mathrm{d}\Phi_{2f} = \frac{|\mathbf{p_t}|}{4\sqrt{s}}\mathrm{d}\Omega_t\,, \tag{25}$$

with $\mathbf{p_t}$ being the momentum and Ω_t the solid angle of the t-quark.

The t-quark and $\bar{t}$-quark decay amplitudes $M_{t\to bW^+}$ and $M_{\bar{t}\to\bar{b}W^-}$, and the corresponding one-loop corrections $\delta M_{t\to bW^+}$ and $\delta M_{\bar{t}\to\bar{b}W^-}$ can be decomposed in terms of the invariant amplitudes

$$\begin{aligned} \mathcal{M}_{t,1}^{(\sigma)} &= \bar{u}(k_3)\not{\varepsilon}(k_{W^+})P_\sigma u(k_t)\,,\\ \mathcal{M}_{\bar{t},1}^{(\sigma)} &= \bar{v}(k_{\bar{t}})\not{\varepsilon}(k_{W^-})P_\sigma v(k_6)\,,\\ \mathcal{M}_{t,2}^{(\sigma)} &= k_t\cdot\varepsilon(k_{W^+})\bar{u}(k_3)P_\sigma u(k_t)\,.\\ \mathcal{M}_{\bar{t},2}^{(\sigma)} &= -k_{\bar{t}}\cdot\varepsilon(k_{W^-})\bar{v}(k_{\bar{t}})P_\sigma v(k_6)\,. \end{aligned} \tag{26}$$

where $P_\sigma=(1+\sigma\gamma_5)/2$ and $\sigma=\pm1$ are the chirality projectors and we have used real polarization vectors for W bosons. The decomposition reads

$$\begin{aligned} M_{t\to bW^+} &= g_{Wff}\mathcal{M}_{t,1}^{(-)}\,,\\ M_{\bar{t}\to\bar{b}W^-} &= g_{Wff}\mathcal{M}_{\bar{t},1}^{(-)}\,,\\ \delta M_{t\to bW^+} &= g_{Wff}\sum_{\substack{i=1,2\\ \sigma=\pm1}} F_{t,i}^{(\sigma)}\mathcal{M}_{t,i}^{(\sigma)}\,,\\ \delta M_{\bar{t}\to\bar{b}W^-} &= g_{Wff}\sum_{\substack{i=1,2\\ \sigma=\pm1}} F_{\bar{t},i}^{(\sigma)}\mathcal{M}_{\bar{t},i}^{(\sigma)}\,. \end{aligned} \tag{27}$$

In (27), g_{Wff} is the SM W boson coupling to fermions which, similarly to the Born form factors of (18), is defined in terms of the effective electric charge e_W

$$g_{Wff} = -\frac{e_W}{\sqrt{2}\sin\theta_W}, \tag{28}$$

$F_{t,i}^{(\sigma)}$ and $F_{\bar{t},i}^{(\sigma)}$ are the EW one-loop form factors of the top quark and antitop quark decay, respectively. The form factors $F_{t,i}^{(\sigma)}$ are calculated numerically with a newly written dedicated subroutine that reproduces the results of [6,7]. The one-loop form factors of the antitop decay are then obtained assuming $\mathcal{CP}$ conservation which lead to the following relations

$$F_{\bar{t},1}^{(\sigma)} = F_{t,1}^{(\sigma)^*}\,,\quad F_{\bar{t},2}^{(\sigma)} = F_{t,2}^{(-\sigma)^*}\,. \tag{29}$$

Note that the imaginary parts of the form factors do not contribute at the one-loop order.

Similarly the W^+-boson and W^--boson decay amplitudes $M_{W^+\to f_1\bar{f}'_1}$ and $M_{W^-\to f_2\bar{f}'_2}$, and the corresponding one-loop corrections $\delta M_{W^+\to f_1\bar{f}'_1}$ and $\delta M_{W^-\to f_2\bar{f}'_2}$ are given by

$$\begin{aligned}
M_{W^+\to f_1\bar{f}'_1} &= g_{Wff}\mathcal{M}^{(-)}_{W^+,1}\,,\\
M_{W^-\to f_2\bar{f}'_2} &= g_{Wff}\mathcal{M}^{(-)}_{W^-,1}\,,\\
\delta M_{W^+\to f_1\bar{f}'_1} &= g_{Wff}\sum_{\substack{i=1,2\\ \sigma=\pm1}} F^{(\sigma)}_{W^+,i}\mathcal{M}^{(\sigma)}_{W^+,i}\,,\\
\delta M_{W^-\to f_2\bar{f}'_2} &= g_{Wff}\sum_{\substack{i=1,2\\ \sigma=\pm1}} F^{(\sigma)}_{W^-,i}\mathcal{M}^{(\sigma)}_{W^-,i}\,,
\end{aligned} \tag{30}$$

with the invariant amplitudes

$$\begin{aligned}
\mathcal{M}^{(\sigma)}_{W^+,1} &= \bar{u}(k_4)\not{\varepsilon}(k_{W^+})P_\sigma v(k_5)\,,\\
\mathcal{M}^{(\sigma)}_{W^-,1} &= \bar{u}(k_7)\not{\varepsilon}(k_{W^-})P_\sigma v(k_8)\,,\\
\mathcal{M}^{(\sigma)}_{W^+,2} &= k_4\cdot\varepsilon(k_{W^+})\bar{u}(k_4)P_\sigma v(k_5)\,.\\
\mathcal{M}^{(\sigma)}_{W^-,2} &= -k_8\cdot\varepsilon(k_{W^-})\bar{u}(k_7)P_\pm v(k_8)
\end{aligned} \tag{31}$$

and the EW one-loop form factors of the W-boson decays $F^{(\sigma)}_{W^\pm,i}$ being calculated numerically, this time with a new subroutine that reproduces the results of [7, 21] for the EW corrected W-boson width. Again, the imaginary parts of the form factors do not contribute at the one-loop order.

The calculation of the EW factorizable corrections to reaction (2) in the pole approximation makes sense only if the invariant masses

$$m_{345} = \sqrt{(p_3+p_4+p_5)^2}\,,\quad m_{678} = \sqrt{(p_6+p_7+p_8)^2} \tag{32}$$

of $bf_1\bar{f}'_1$ and $\bar{b}f_2\bar{f}'_2$ are close to m_t, and if

$$m_{45} = \sqrt{(p_4+p_5)^2}\,,\quad m_{78} = \sqrt{(p_7+p_8)^2} \tag{33}$$

of $f_1\bar{f}'_1$ and $f_2\bar{f}'_2$ do not depart too much from m_W. Otherwise, the signal diagrams of Fig. 1a stop to dominate the cross section and the association of the reduced phase space point, at which the EW factorizable $\mathcal{O}(\alpha)$ corrections depicted in Fig. 2 are calculated, with the phase space point of the full six particle phase space of (2) may lead to unnecessary distortion of the off-resonance background contributions. Therefore, in the following, we will impose kinematical cuts on the quantities

$$\begin{aligned}
&\delta_t = m_{345}/m_t - 1\,,\quad \delta_{\bar{t}} = m_{678}/m_t - 1\,,\\
&\delta_{W^+} = m_{45}/m_W - 1\,,\quad \delta_{W^-} = m_{78}/m_W - 1\,,
\end{aligned} \tag{34}$$

which describe the relative departures of the invariant masses of (32) and (33) from m_t and m_W, respectively.

3 Numerical results

In this section, we will illustrate the effect of the factorizable EW $\mathcal{O}(\alpha)$ corrections described in Sect. 2 on the SM predictions for six fermion reactions relevant for detection of the top quark pair production and decay at the ILC (2) by showing results for total cross sections of its two specific channels (3) and (4).

We choose the Z boson mass, Fermi coupling and fine structure constant in the Thomson limit as the EW SM input parameters

$$\begin{aligned}
&m_Z = 91.1876\,\text{GeV}\,,\quad G_\mu = 1.16637\times10^{-5}\,\text{GeV}^{-2}\,,\\
&\alpha_0 = 1/137.0359895\,.
\end{aligned} \tag{35}$$

The external fermion masses of reaction (3) and the top quark mass are the following:

$$\begin{aligned}
&m_e = 0.51099907\,\text{MeV}\,,\quad m_\mu = 105.658389\,\text{MeV}\,,\\
&m_b = 4.7\,\text{GeV}\,,\quad m_t = 178\,\text{GeV}\,.
\end{aligned} \tag{36}$$

For definiteness, we give also values of the other fermion masses

$$\begin{aligned}
&m_\tau = 1.77705\,\text{GeV}\,,\quad m_u = 75\,\text{MeV}\,,\quad m_d = 75\,\text{MeV}\,,\\
&m_s = 250\,\text{MeV}\,,\quad m_c = 1.5\,\text{GeV}
\end{aligned} \tag{37}$$

and the value of a strong coupling $\alpha_s(m_Z^2) = 0.117$.

Assuming a value of the Higgs boson mass, the W boson mass and the Z boson width are determined with ZFITTER [40], while the SM Higgs boson width is calculated with HDECAY [41]. We obtain the following values of these parameters for $m_H = 120\,\text{GeV}$:

$$\begin{aligned}
&m_W = 80.38509\,\text{GeV}\,,\quad \Gamma_Z = 2.495270\,\text{GeV}\,,\\
&\Gamma_H = 3.2780\,\text{MeV}\,.
\end{aligned} \tag{38}$$

The actual values of the Z and Higgs boson widths are not very relevant in the context of the top quark pair production, as they enter the calculation through the off-resonance background contributions. The EW corrected top quark and W boson widths, which on the other hand play an essential role for the calculation, are calculated with a newly written dedicated subroutine that reproduces the results of [7, 21]. We obtain the following values for them for the parameters specified in (35)–(37)

$$\Gamma_W = 2.03777\,\text{GeV}\,,\quad \Gamma_t = 1.67432\,\text{GeV}\,. \tag{39}$$

We have neglected the QCD correction to the widths Γ_W and Γ_t, as no QCD corrections have been included in the one-loop corrections to the $t\bar{t}$-pair production process. The EW corrected widths of (39) are used in the calculation of the cross sections that include the EW factorizable corrections. For the calculation of the lowest order cross sections of (3) and (4), the corresponding lowest order SM values of the top quark and W-boson widths are used.

Results for the total cross sections of reactions (3) and (4) at three different centre of mass (CMS) energies in the presence of the following cuts on quantities $\delta_t, \delta_{\bar{t}}, \delta_{W^+}, \delta_{W^-}$, defined in (34),

$$\delta_t < 0.1, \delta_{\bar{t}} < 0.1, \delta_{W^+} < 0.1, \delta_{W^-} < 0.1\,, \qquad (40)$$

are shown in Table 1. The second column shows the Born cross section calculated with the complete set of the lowest order Feynman diagrams. The third column shows the Born 'signal' cross section, i.e. the cross section obtained with the two lowest order signal diagrams of Fig. 1a only. We see that imposing the invariant mass cuts (40) efficiently reduces the off-resonance background, which becomes quite sizeable if the cuts are not imposed [23, 42]. The fourth and fifth columns show the cross sections including the ISR and factorizable EW corrections separately and the sixth column shows the results including both the ISR and EW factorizable corrections. Note that the cross sections of (4) are almost exactly three times larger than the cross sections of (3), in agreement with the naive counting of the colour degrees of freedom. This is because the neutral current off-resonance background contributions that make reaction (3) differ from (4) are almost completely suppressed in the presence of cuts (40).

How the radiative corrections for the six fermion reactions (2) depend on the CMS energy is illustrated in Fig. 3, where, on the left-hand side, we plot the total cross sections of reaction (4) as a function of the CMS energy, both in the lowest order and including different classes of corrections. The dashed-dotted line shows the Born cross section, the dotted line is the cross section including the ISR correction, the dashed line shows the effect of the factorizable EW correction, while the solid line shows the effect of the combined ISR and factorizable EW corrections. The plots on the right-hand side of Fig. 3 show the corresponding relative corrections

$$\delta_{\text{cor.}} = \frac{\sigma_{\text{Born+cor.}} - \sigma_{\text{Born}}}{\sigma_{\text{Born}}}\,,\ \text{cor.} = \text{FEW, ISR, ISR+FEW.} \qquad (41)$$

Table 1. Total cross sections of reactions (3) and (4) in fb at three different CMS energies in the presence of cuts (40). The numbers in parenthesis show the uncertainty of the last decimals

		$e^+e^- \to b\nu_\mu\mu^+\bar{b}\mu^-\bar{\nu}_\mu$			
$\sqrt{s}$ (GeV)	σ_{Born}	$\sigma^{t^*\bar{t}^*}_{\text{Born}}$	$\sigma_{\text{Born+ISR}}$	$\sigma_{\text{Born+FEWC}}$	$\sigma_{\text{Born+ISR+FEWC}}$
430	5.9117(54)	5.8642(45)	5.2919(91)	5.6884(55)	5.0978(53)
500	5.3094(50)	5.2849(43)	5.0997(51)	4.9909(49)	4.8085(48)
1000	1.6387(16)	1.6369(15)	1.8320(18)	1.4243(14)	1.6110(16)
		$e^+e^- \to b\nu_\mu\mu^+\bar{b}d\bar{u}$			
$\sqrt{s}$ (GeV)	σ_{Born}	$\sigma^{t^*\bar{t}^*}_{\text{Born}}$	$\sigma_{\text{Born+ISR}}$	$\sigma_{\text{Born+FEWC}}$	$\sigma_{\text{Born+ISR+FEWC}}$
430	17.727(16)	17.592(13)	15.857(20)	17.052(16)	15.283(16)
500	15.950(15)	15.855(13)	15.311(15)	14.977(16)	14.438(14)
1000	4.9134(48)	4.9106(46)	5.4949(55)	4.2697(40)	4.8287(47)

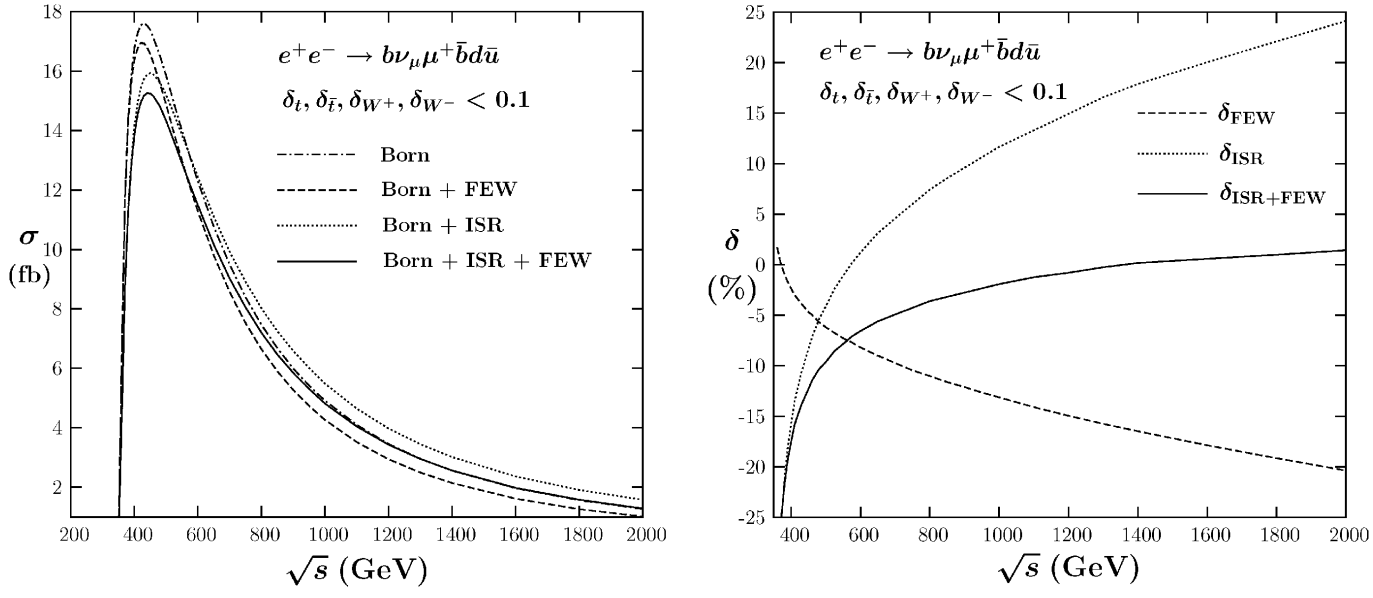

Fig. 3. Total cross sections of (4) including different classes of the SM radiative corrections (*left*) and corresponding relative corrections (41) (*right*) as functions of the CMS energy

The dashed line shows the relative factorizable EW correction. The correction is small and positive, a few GeV above the $t\bar{t}$-pair production threshold, but already about 20 GeV above the threshold it becomes negative and it falls down logarithmically towards more and more negative values, due to the large logarithmic terms $\sim \left[\ln\left(m_W^2/s\right)\right]^2$ and $\sim \ln\left(m_W^2/s\right)$, reaching 20% at $\sqrt{s} = 2$ TeV. The dotted line shows the relative ISR correction, which on the other hand, is dominated by the large collinear logarithms $\left[\ln\left(s/m_e^2\right)\right]^2$ and $\ln\left(s/m_e^2\right)$. It starts from about -25% at energies close to the threshold and grows to almost $+25\%$ at $\sqrt{s} = 2$ TeV. Finally, the solid line shows the combined ISR and factorizable EW correction. The net relative correction is dominated by the ISR: it is large and negative for energies not far above the threshold and it becomes positive at high energies, reaching 1.4% at $\sqrt{s} = 2$ TeV.

4 Summary and outlook

We have calculated the SM predictions for top quark pair production and decay into six fermions at a linear e^+e^- collider. We have included the factorizable EW $\mathcal{O}(\alpha)$ corrections in the pole approximation and QED corrections due to the initial state radiation in the structure function approach into SM predictions for the top quark pair production and decay into six fermions at ILC. We have illustrated the effect of the radiative corrections on the predictions by showing numerical results for two selected six-fermion reactions (3) and (4). The ISR and factorizable EW radiative corrections are sizeable and, therefore, should be included in the analysis of future precision data on the top quark pair production and decay from ILC.

In order to obtain a complete EW next-to-leading order result for the six fermion reactions (2) in the pole approximation, one should include the nonfactorizable virtual photonic corrections corresponding to an exchange of a virtual photon between the electrically charged lines of the signal diagrams of Fig. 1a, which have not been included in the shaded blobs of Fig. 2. For example, the exchange of a photon between the initial state electron and any of the final state fermions or intermediate W bosons, or between the b and $\bar{t}$ quarks, or its decay products, should be taken into account. This would allow for inclusion of the real photon emission from the external legs in an exclusive way. Taking into account the QCD corrections would also be highly desirable.

Acknowledgements. K. Kołodziej is grateful to the Alexander von Humboldt Foundation for supporting his stay at DESY, Zeuthen, where this work was partly carried out and to the DESY Theory Group, Zeuthen, for the kind hospitality.

Appendix : Projection of momenta

In this appendix, we describe the projection procedure used in order to associate each phase space point of the full six-particle phase space of reaction (2) with a point of the reduced phase space of the on-shell top pair production (1) and subsequent decay. The on-shell momenta k_t and $k_{\bar{t}}$ of the t-quark and $\bar{t}$-antiquark, $k_{W^\pm}$ of the decay $W^\pm$-bosons, and k_i, $i = 3, \ldots, 8$, of the decay fermions of reaction (2) are constructed from the four momenta p_i, $i = 3, ..., 8$, of the final state fermions of reaction (2) with the following projection procedure.

First, the on-shell four momenta of t and $\bar{t}$ in the CMS are found in the following way

$$
\begin{aligned}
&|\mathbf{k}_t| = \frac{\lambda^{\frac{1}{2}}\left(s, m_t^2, m_t^2\right)}{2s^{\frac{1}{2}}}\,, \qquad \mathbf{k}_t = |\mathbf{k}_t|\,\frac{\mathbf{p}_3+\mathbf{p}_4+\mathbf{p}_5}{|\mathbf{p}_3+\mathbf{p}_4+\mathbf{p}_5|}\,,\\
&k_t^0 = \left(\mathbf{k}_t^2 + m_t^2\right)^{\frac{1}{2}}\,, \qquad\qquad \mathbf{k}_{\bar{t}} = -\mathbf{k}_t, k_{\bar{t}}^0 = \sqrt{s} - k_t^0\,.
\end{aligned}
\tag{A.1}
$$

Then the four momenta p_3, p_4 and p_5 (p_6, p_7 and p_8) are boosted to the rest frame of the $bf_1\bar{f}_1'$ ($\bar{b}f_2\bar{f}_2'$) subsystem of reaction (2), where they are denoted p_3', p_4' and p_5' (p_6', p_7' and p_8'). The projected four momenta k_3' of b (k_6' of $\bar{b}$) is determined in the rest frame of $bf_1\bar{f}_1'$ ($\bar{b}f_2\bar{f}_2'$) according to

$$
\begin{aligned}
&|\mathbf{k'}_i| = \frac{\lambda^{\frac{1}{2}}\left(m_t^2, m_i^2, m_W^2\right)}{2m_t}\,, \quad \mathbf{k'}_i = |\mathbf{k'}_i|\,\frac{\mathbf{p'}_i}{|\mathbf{p'}_i|}\,,\\
&k'^0_i = \left(\mathbf{k'}^2_i + m_i^2\right)^{\frac{1}{2}}\,, \quad i = 3, 6\,,
\end{aligned}
\tag{A.2}
$$

which means that the directions of the b and $\bar{b}$ momenta are kept unchanged while their lengths are being altered.

The four momenta p_4' and p_5' (p_7' and p_8') are further boosted to the rest frame of $f_1\bar{f}_1'$ ($f_2\bar{f}_2'$), where they are denoted p_4'' and p_5'' (p_7'' and p_8''). The projected four momenta k_4'' and k_5'' of f_1 and $\bar{f}_1'$ (k_7'' and k_8'' of f_2 and $\bar{f}_2'$) are in this frame determined according to

$$
\begin{aligned}
&|\mathbf{k'}_4| = \frac{\lambda^{\frac{1}{2}}\left(m_W^2, m_4^2, m_5^2\right)}{2m_W}\,, \quad |\mathbf{k'}_7| = \frac{\lambda^{\frac{1}{2}}\left(m_W^2, m_7^2, m_8^2\right)}{2m_W}\,,\\
&\mathbf{k''}_i = |\mathbf{k''}_i|\,\frac{\mathbf{p''}_i}{|\mathbf{p''}_i|}\,, \quad i = 4, 7,\\
&\mathbf{k''}_5 = -\mathbf{k''}_4\,, \quad \mathbf{k''}_8 = -\mathbf{k''}_7\,,\\
&k''^0_j = \left(\mathbf{k''}^2_j + m_j^2\right)^{\frac{1}{2}}\,, \quad j = 4, 5, 7, 8\,.
\end{aligned}
\tag{A.3}
$$

This again means that the directions of momenta of f_1, $\bar{f}_1'$, f_2 and $\bar{f}_2'$ are kept unchanged while their lengths are being altered.

The four momenta k_4'' and k_5'' (k_7'' and k_8'') are now boosted to the rest frame of the on-shell t ($\bar{t}$) and, finally, k_3', k_4' and k_5' (k_6', k_7' and k_8') are boosted from the t ($\bar{t}$) rest frame to the CMS giving the desired projected four momenta k_i, $i = 3, \ldots, 8$. As one can easily see from (A.1)–(A.3), the projected momenta, except for satisfying the necessary on-shell relations $k_i^2 = m_i^2$, $i = 3, \ldots, 8$, also fulfill other required on-shell relations

$$
\begin{aligned}
&(k_3 + k_4 + k_5)^2 = (k_6 + k_7 + k_8)^2 = m_t^2\,,\\
&(k_4 + k_5)^2 = (k_7 + k_8)^2 = m_W^2\,.
\end{aligned}
\tag{A.4}
$$

Table 2. A comparison of two randomly selected sets of the four momenta p_i, $i = 3, \ldots, 8$, $p_3 + p_4 + p_5$, $p_6 + p_7 + p_8$, $p_4 + p_5$, $p_7 + p_8$ and their projections k_i, $i = 3$, ..., 8, k_t, $k_{\bar{t}}$, k_{W^+}, k_{W^-}, respectively. Quantities $\delta_t = m_{345}/m_t - 1$, $\delta_{\bar{t}} = m_{678}/m_t - 1$, $\delta_{W^+} = m_{45}/m_W - 1$ and $\delta_{W^-} = m_{78}/m_W - 1$ describe relative departures of the corresponding final state particle subsystems from a mass-shell of t, $\bar{t}$, W^+ and W^-, respectively

GeV	$\delta_t = 0.03\%$, $\delta_{\bar{t}} = 0.19\%$, $\delta_{W^+} = 0.26\%$, $\delta_{W^-} = 0.85\%$				$\delta_t = 0.06\%$, $\delta_{\bar{t}} = 0.17\%$, $\delta_{W^+} = 0.78\%$, $\delta_{W^-} = 3.23\%$			
p_3	154.0	141.4	–28.1	53.8	116.5	89.3	13.1	73.6
k_3	153.8	141.3	–28.0	53.8	116.9	89.6	13.1	73.8
p_4	22.9	–15.1	–7.7	–15.4	117.6	92.8	–20.6	–69.3
k_4	22.9	–15.0	–7.8	–15.4	117.4	92.5	–20.6	–69.2
p_5	73.1	24.6	35.7	58.8	16.0	–3.2	7.5	13.8
k_5	73.3	24.8	35.8	59.0	15.7	–3.3	7.5	13.5
p_6	64.5	–10.0	57.5	–27.0	109.8	–78.5	–12.1	–75.7
k_6	64.0	–10.0	57.1	–26.9	108.1	–77.2	–11.9	–74.6
p_7	112.1	–109.2	–20.7	–15.1	106.1	–95.4	33.7	32.0
k_7	112.4	–109.5	–20.4	–15.1	107.8	–97.2	34.5	31.4
p_8	73.5	–31.7	–36.8	–55.1	33.9	–4.9	–21.6	25.7
k_8	73.6	–31.5	–36.7	–55.5	34.1	–4.4	–22.6	25.1
$p_3 + p_4 + p_5$	249.9	150.9	0.0	97.3	250.1	178.9	0.0	18.0
k_t	250.0	151.0	0.0	97.4	250.0	178.8	0.0	18.0
$p_6 + p_7 + p_8$	250.1	–150.9	0.0	–97.3	249.9	–178.9	0.0	–18.0
$k_{\bar{t}}$	250.0	–151.0	0.0	–97.4	250.0	–178.8	0.0	–18.0
$p_4 + p_5$	95.9	9.5	28.1	43.5	133.6	89.6	–13.1	–55.5
k_{W^+}	96.2	9.8	28.0	43.6	133.1	89.2	–13.1	–55.8
$p_7 + p_8$	185.6	–140.9	–57.5	–70.3	140.0	–100.4	12.1	57.7
k_{W^-}	186.0	–141.0	–57.1	–70.5	141.9	–101.6	11.9	56.6

The described projection procedure is not unique. Moreover, it strongly depends on the departures (34) of invariant masses m_{345}, m_{678} of (32) from m_t, and of the invariant masses m_{45}, m_{78} of (33) from m_W. How it works in practice is illustrated in Table 2, where two randomly selected sets of four momenta p_i, $i = 3, \ldots 8$, $p_3 + p_4 + p_5$, $p_6 + p_7 + p_8$, $p_4 + p_5$, $p_7 + p_8$, and their projections k_i, $i = 3$, ..., 8, k_t, $k_{\bar{t}}$, k_{W^+}, k_{W^-}, respectively, are compared. Momenta p_i have been generated according to the Breit–Wigner distribution in such a way that the invariant masses of the $bf_1\bar{f}_1'$, $\bar{b}f_2\bar{f}_2'$, $f_1\bar{f}_1'$ and $f_2\bar{f}_2'$ subsystems of reaction (2) fall into the vicinity of the masses of the corresponding primary on-shell particles: t-quark, $\bar{t}$-antiquark, W^+-boson and W^--boson, respectively.

References

1. ECFA/DESY LC Physics Working Group Collaboration, J.A. Aguilar-Saavedra et al., arXiv:hep-ph/0106315; American Linear Collider Working Group Collaboration, T. Abe et al., arXiv:hep-ex/0106056; ACFA Linear Collider Working Group Collaboration, K. Abe et al., arXiv:hep-ph/0109166
2. V.S. Fadin, V.A. Khoze, JETP Lett. **46**, 525 (1987); Sov. J. Nucl. Phys. **48**, 309 (1988); M.J. Strassler, M.E. Peskin, Phys. Rev. D **43**, 1500 (1991); M. Jeżabek, J.H. Kühn, T. Teubner, Z. Phys. C **56**, 653 (1992); Y. Sumino, K. Fuji, K. Hagiwara, M. Murayama, C.K. Ng, Phys. Rev. D **47**, 56 (1992)
3. A.H. Hoang, T. Teubner, Phys. Rev. D **58**, 114023 (1998), Phys. Rev. D **60**, 114027 (1999); K. Melnikov, A. Yelkhovsky, Nucl. Phys. B **528**, 59 (1998); O. Yakovlev, Phys. Lett. B **457**, 170 (1999); M. Beneke, A. Signer, V. Smirnov, Phys. Lett. B **454**, 137 (1999); T. Nagano, A. Ota, Y. Sumino, Phys. Rev. D **60**, 114014 (1999); A.H. Hoang, A.V. Manohar, I.W. Stewart, T. Teubner, Phys. Rev. Lett. **86**, 1951 (2001), [hep-ph/0107144]; A.A. Penin, A.A. Pivovarov, Phys. Atom. Nucl. **64**, 275 (2001); A.H. Hoang et al., Eur. Phys. J. Direct C **3**, 1 (2000)
4. D. Peralta, M. Martinez, R. Miquel, Top Mass Measurement at the $t\bar{t}$ Threshold. In: Proc. Int. Workshop on Linear Colliders (LCWS99), Sitges, May (1999)
5. M. Jeżabek, J.H. Kühn, Nucl. Phys. B **314**, 1 (1989); G. Eilam, R.R. Mendel, R. Migneron, A. Soni, Phys. Rev. Lett. **66**, 3105 (1991)
6. A. Denner, T. Sack, Nucl. Phys. B **358**, 46 (1991)
7. A. Denner, Fortsch. Phys. **41**, 307 (1993)
8. A. Czarnecki, K. Melnikov, Nucl. Phys. B **544**, 520 (1999); K.G. Chetyrkin, R. Harlander, T. Seidensticker, M. Steinhauser, Phys. Rev. D **60**, 114015 (1999)
9. K.G. Chetyrkin, J.H. Kühn, M. Steinhauser, Nucl. Phys. B **482**, 213 (1996); R. Harlander, M. Steinhauser, Eur. Phys. J. C **2**, 151 (1998)
10. B. Grządkowski et al., Nucl. Phys. B **281**, 18 (1987); W. Beenakker, S.C. van der Marck, W. Hollik, Nucl Phys. B **365**, 24 (1991); R.J. Guth, J.H. Kühn, Nucl. Phys. B **368**, 38 (1992); W. Beenakker, A. Denner, A. Kraft, Nucl. Phys. B **410**, 219 (1993); V. Driesen, W. Hollik, A. Kraft, hep-ph/9603398; In: e^+e^- Collisions at TeV Energies: The Physics Potential, Proc. Workshop, Annecy, Gran

Sasso, Hamburg, February 1995, September 1995, ed. by P.M. Zerwas, DESY 96–123D, 33 (1996)
11. J. Fleischer, A. Leike, T. Riemann, A. Werthenbach, Eur. Phys. J. C **31**, 37 (2003), [hep-ph/0302259]; J. Fleischer, A. Leike, A. Lorca, T. Riemann, A. Werthenbach, Fortran program topfit v.0.93 (10 June 2003); available at http://www-zeuthen.desy.de/theory/research
12. A. Lorca, T. Riemann, Comput. Phys. Commun. **174**, 71 (2006) [hep-ph/0412047]; A. Biernacik, K. Kolodziej, A. Lorca, T. Riemann, Acta Phys. Polon. B **34**, 5487 (2003), [hep-ph/0311097]; A. Lorca, DESY-THESIS-2005-004
13. A.A. Akhundov, D.Yu. Bardin, A. Leike, Phys. Lett. B **261**, 321 (1991)
14. R.J. Guth, J.H. Kühn, Nucl. Phys. B **368**, 38 (1992)
15. J. Jersak, E. Laerman, P.M. Zerwas, Phys. Rev. D **25**, 1218 (1982); Erratum Phys. Rev. D **36**, 310 (1987)
16. J.H. Kühn, T. Hahn, R. Harlander, hep-ph/9912262
17. J. Fleischer, J. Fujimoto, T. Ishikawa, A. Leike, T. Riemann, Y. Shimizu, A. Werthenbach, In: KEK Proc. 2002-11 ed. by Y. Kurihara (2002), p. 153 [hep-ph/0203220]
18. T. Hahn, W. Hollik, A. Lorca, T. Riemann, A. Werthenbach, hep-ph/0307132
19. D. Bardin, S. Riemann, T. Riemann, Z. Phys. C **32**, 121 (1986)
20. F. Jegerlehner, In: Proc. XI Int. School of Theoretical Phys., ed. by M. Zrałek, R. Mańka (World Scientific, 1988), pp. 33–108
21. A. Denner, T. Sack, Z. Phys. C **46**, 653 (1990)
22. K. Kołodziej, Eur. Phys. J. C **23**, 471 (2002), [hep-ph/0110063], Comput. Phys. Commun. **151**, 339 (2003), [hep-ph/0210199]
23. A. Biernacik, K. Kołodziej, Nucl. Phys. Proc. Suppl. **116**, 33 (2003), [hep-ph/0210405]
24. E. Accomando, A. Ballestrero, M. Pizzio, Nucl.Phys. B **512**, 19 (1998); E. Accomando, A. Ballestrero, M. Pizzio, Nucl. Phys. B **547**, 81 (1999)
25. G. Montagna, M. Moretti, O. Nicrosini, F. Piccinini, Eur. Phys. J. C **2**, 483 (1998), [hep-ph/9705333]; F. Gangemi et al., Eur. Phys. J. C **9**, 31 (1999), [hep-ph/9811437], Nucl. Phys. B **559**, 3 (1999), [hep-ph/9905271]; F. Gangemi, hep-ph/0002142
26. S. Dittmaier, M. Roth, Nucl. Phys. B **642**, 307 (2002), [hep-ph/0206070]
27. F. Krauss, R. Kuhn, G. Soff, JHEP **0202**, 044 (2002), [hep-ph/0109036]; A. Schalicke, F. Krauss, R. Kuhn, G. Soff, JHEP **0212**, 013 (2002), [hep-ph/0203259]
28. Minami-Tateya Collaboration, T. Ishikawa et al., KEK-92-19; Minami-Tateya Collaboration, H. Tanaka et al., Nucl. Instrum. Methods A **389**, 295 (1997); F. Yuasa et al., Prog. Theor. Phys. Suppl. **138**, 18 (2000), [hep-ph/0007053]
29. S. Kawabata, Comput. Phys. Commun. **88**, 309 (1995)
30. T. Stelzer, W.F. Long, Comput. Phys. Commun. **81**, 357 (1994), [hep-ph/9401258]; H. Murayama, I. Watanabe, K. Hagiwara, KEK-91-11
31. F. Maltoni, T. Stelzer, JHEP **0302**, 027 (2003), [hep-ph/0208156]
32. C.G. Papadopoulos, Comput. Phys. Commun. **137**, 247 (2001), [hep-ph/0007335]
33. A. Kanaki, C.G. Papadopoulos, Comput. Phys. Commun. **132**, 306 (2000), hep-ph/0002082
34. W. Kilian, LC-TOOL-2001-039
35. A. Pukhov et al., hep-ph/9908288
36. M. Moretti, T. Ohl, J. Reuter, LC-TOOL-2001-040, hep-ph/0102195
37. S. Dittmaier, hep-ph/0308079
38. W. Beenakker et al., In: Physics at LEP2, ed. by G. Altarelli, T. Sjöstrand, F. Zwirner, Report CERN 96-01, Geneva **1**, 79 (1996), [hep-ph/9602351]
39. A. Denner, S. Dittmaier, M. Roth, D. Wackeroth, Nucl. Phys. B **560**, 33 (1999); Comput. Phys. Commun. **153**, 462 (2003)
40. D. Bardin, M. Bilenky, M. Jack, P. Christova, L. Kalinovskaya, A. Olshevsky, S. Riemann, T. Riemann, Comput. Phys. Commun. **133**, 229 (2001), [hep-ph/9908433]; A. Arbuzov, M. Awramik, M. Czakon, A. Freitas, M. Grünewald, K. Mönig, S. Riemann, T. Riemann, hep-ph/0507146, submitted to Comp. Phys. Commun.; see also http://www-zeuthen.desy.de/theory/research/zfitter
41. A. Djouadi, J. Kalinowski, M. Spira, Comput. Phys. Commun. **108**, 56 (1998)
42. K. Kołodziej, Acta Phys. Pol. B **34**, 4511 (2003)